The WFIRST Coronagraph Instrument

John Trauger and the WFIRST CGI development team
Jet Propulsion Laboratory
California Institute of Technology

Mirror Tech Workshop
Raytheon, El Segundo – 7 November 2018

The decision to implement the WFIRST mission will not be finalized until NASA completes the National Environmental Policy Act (NEPA) process. This document is being made available for information purposes only.
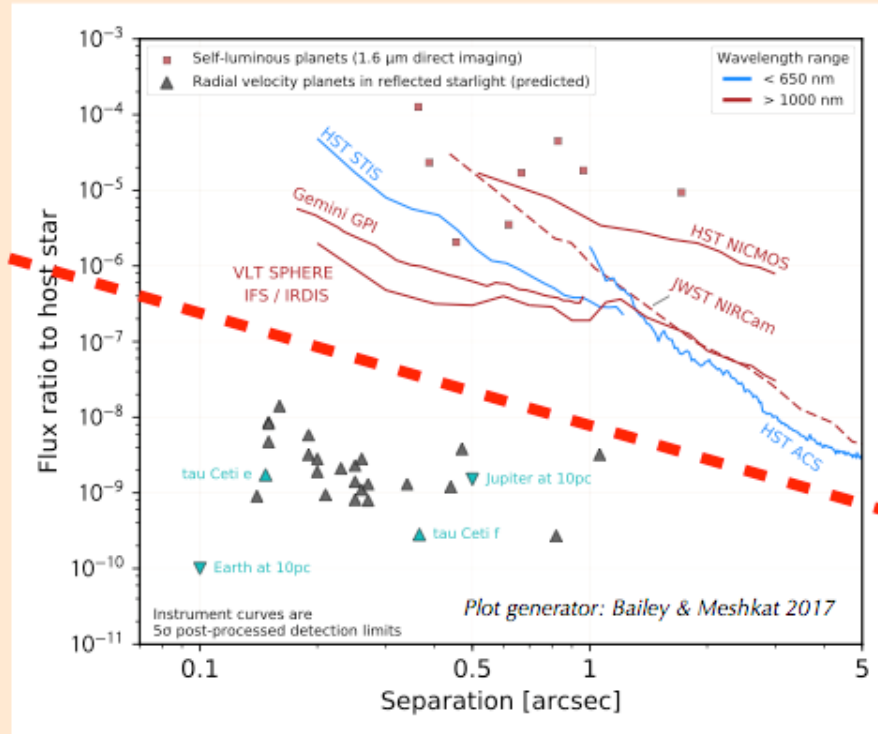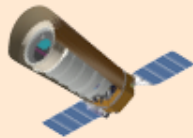
Direct Imaging of Exoplanets: 2018
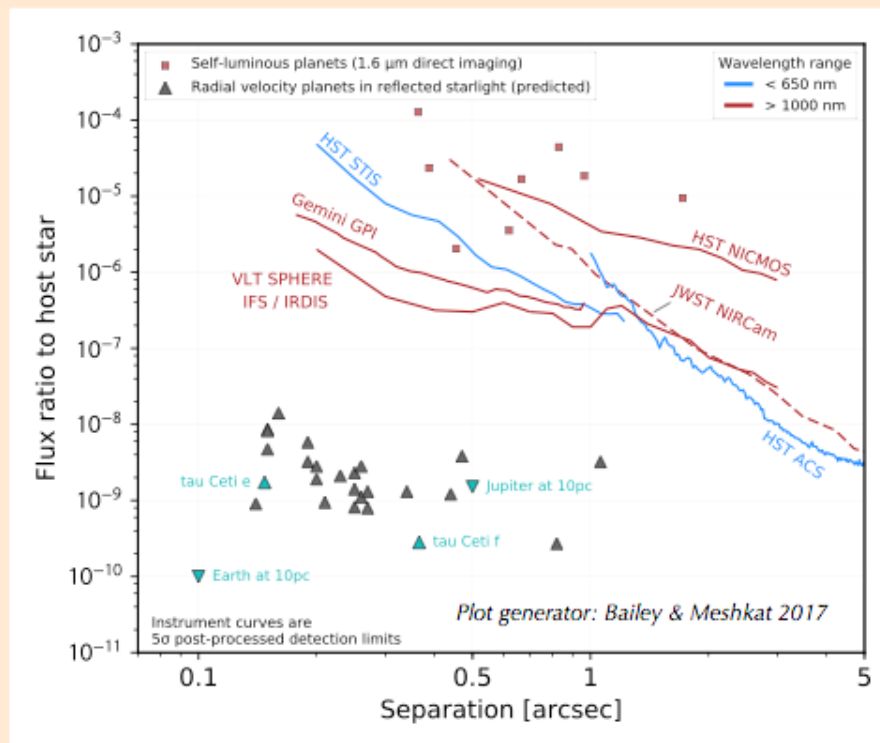
Direct imaging and spectroscopy of **young self-luminous exoplanets** have been achieved from ground and space observatories. Direct imaging of **mature cool exoplanets in reflected starlight** is currently beyond the reach of conventional techniques, as illustrated by the estimated brightness of a sample of known radial velocity exoplanets.

The WFIRST Coronagraph Instrument relies on the stability of a Space Observatory

Ground-based observatory

*Phase-dominated wavefront aberrations: Adaptive wavefront control*

Space observatory

Complex wavefront aberrations: Iterative wavefront control

*Ground-based AO systems correct the rapid phase-dominated wavefront errors due to atmospheric turbulence. Freedom from atmospheric turbulence enables the **iterative correction of both phase and amplitude wavefront aberrations** and the suppression of scattered and diffracted light to levels limited only by telescope and instrument stability.*
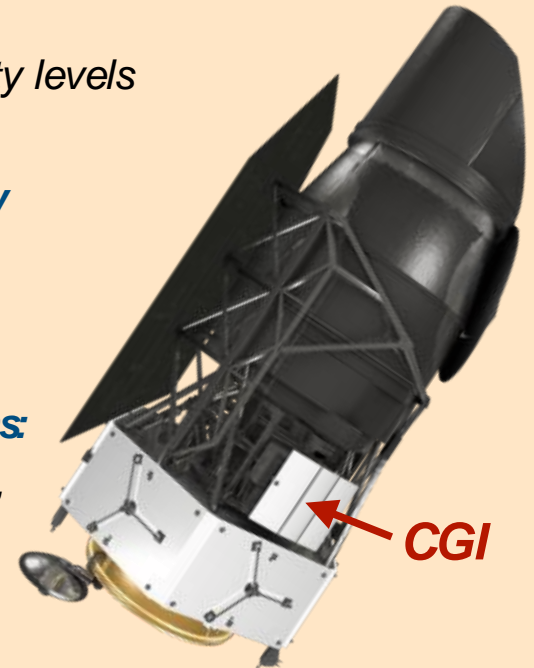
WFIRST-CGI pioneers space coronagraph technologies
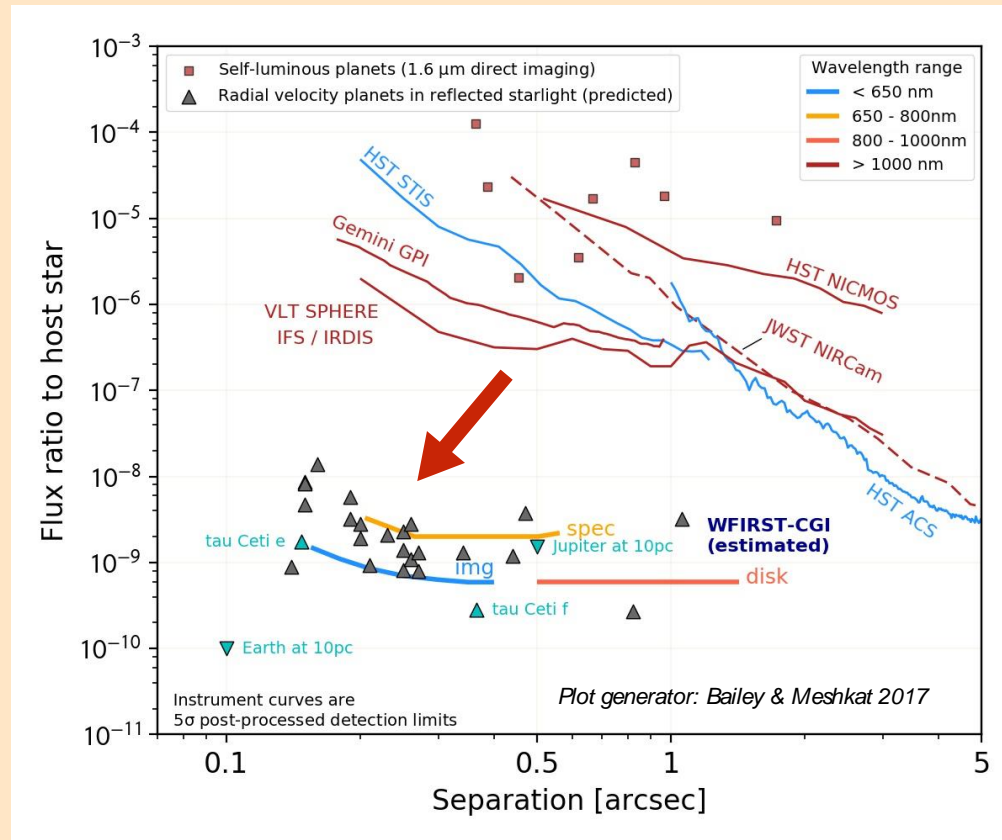
Best estimated CGI performance *for three observing configurations (direct imaging at short and long wavelengths, and integral field spectroscopy) are based on currently demonstrated static and dynamic testbed performance and observatory optical disturbance models provided by the WFIRST project.*

The WFIRST Coronagraph Instrument (CGI)

- **The Coronagraph Instrument (CGI) is one of two instruments on the Wide Field Infrared Survey Telescope (WFIRST)**, *a NASA project now in the design (Phase B) stage and scheduled for launch in 2025.*

- *CGI is designed to* **demonstrate space coronagraphy** *at sensitivity levels of Jovian-mass planets and faint debris disks in reflected starlight.*

- *The* **CGI design is tailored to the predicted WFIRST observatory characteristics***, and design refinements continue as engineering knowledge of the WFIRST advances.*

- *The CGI will demonstrate in space, for the first time,* **key enabling technologies for future exo-Earth imaging missions***:*
    - *precision optical* **wavefront control** *with deformable mirrors,*
    - *sensitive* **EMCCD photon-counting** *imaging detectors,*
    - **selectable coronagraph** *observing modes,*
    - *low-resolution* **integral field spectroscopy,**
    - **advanced algorithms** *for wavefront sensing and control,*
    - **high-fidelity models** *for the integrated spacecraft and coronagraph,*
    - *and* **post-processing methods** *to extract images and spectra.*

CGI

WFIRST
WIDE-FIELD INFRARED SURVEY TELESCOPE
DARK ENERGY • EXOPLANETS • ASTROPHYSICS

The Coronagraph Instrument on WFIRST is an advanced technology demonstrator for future missions aiming to directly image Earth-like exoplanets.
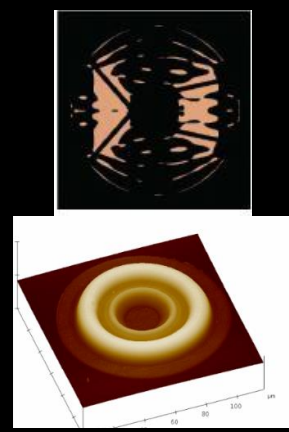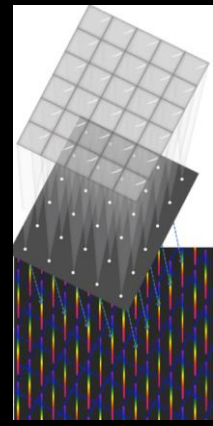
Autonomous Ultra-Precise Wavefront Sensing & Control
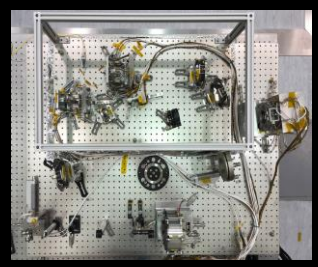
Large-format Deformable Mirrors

High-contrast Coronagraph Masks

High-contrast Integral Field Spectroscopy

Ultra-low noise photon counting EMCCD Detectors
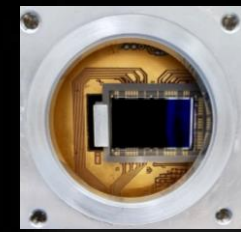
Data Post-Processing
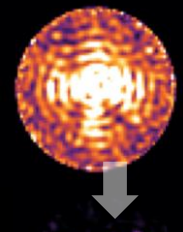
CGI will demonstrate for the first time in space the technologies needed to image and characterize rocky planets in the habitable zones of nearby stars. By demonstrating these tools in an integrated end-to-end system and enabling scientific observing operations, NASA will validate performance models and provide the pathway for potential future flagship missions.

CGI optical bench

FSM

DM 2

DM 1

DM electronics

Structural frame

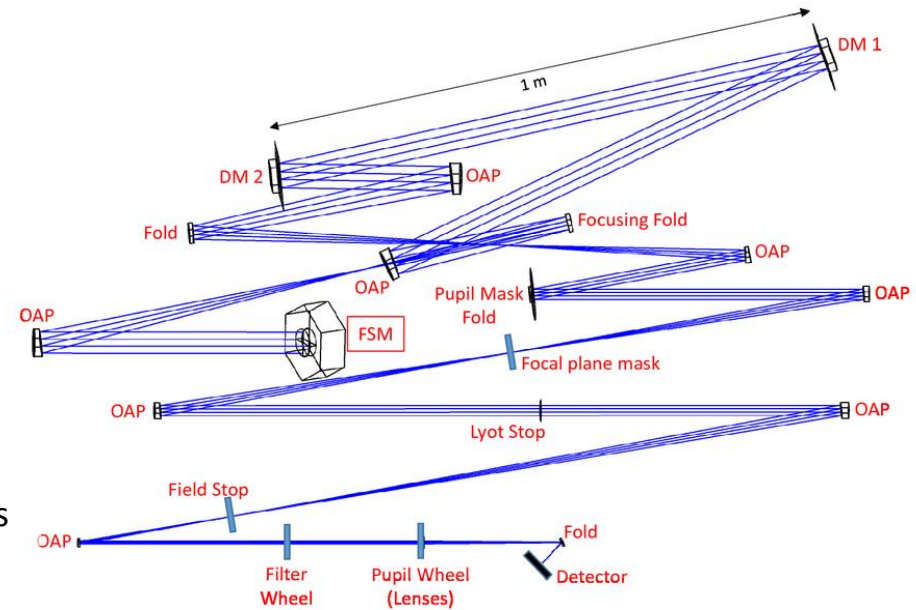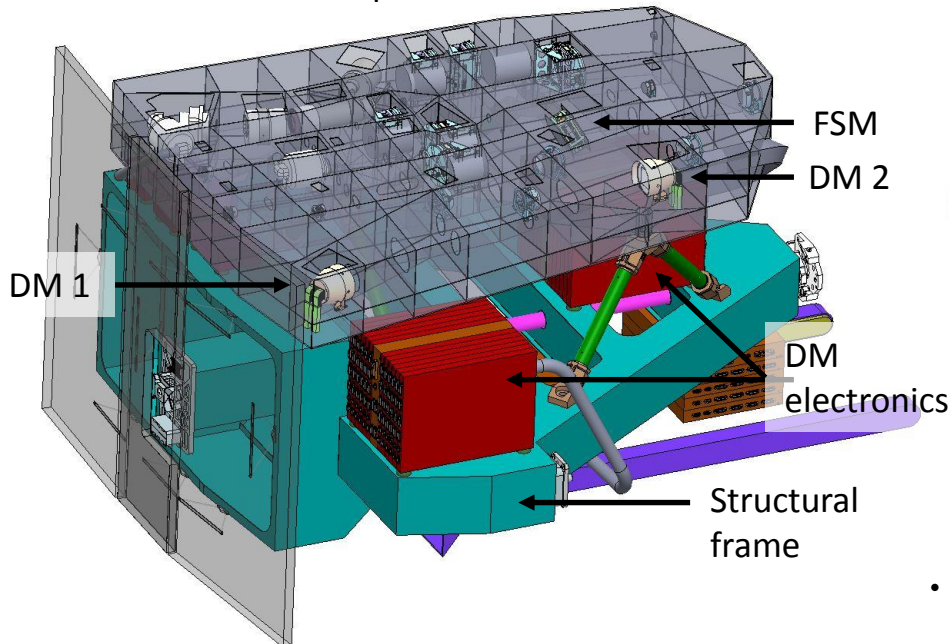- In the WFIRST Payload, CGI mounts onto the Instrument Carrier (IC) shared with the Wide Field Instrument. The Tertiary Collimator Assembly (TCA; not shown) is the optical interface between the telescope and CGI, and relays an exit pupil onto the Fast Steering Mirror (FSM).
- Phase A design as of May 2018.

- The first deformable mirror, **DM 1**, is positioned at a relay pupil following the **FSM**. **DM 2** is positioned 1 meter away to enable correction of amplitude errors and phase errors originating from out-of-pupil surfaces.
- Both coronagraph mask types, the Hybrid Lyot and Shaped Pupil Coronagraphs (HLC and SPC), are implemented on the same optical beam train and selected by changing masks at the planes labeled **Pupil Mask Fold**, **Focal plane mask**, and **Lyot Stop**.
- The filter and the camera channel (either the Direct Imaging Camera or the Integral Field Spectrograph) are selected by mechanisms after the Lyot stop.
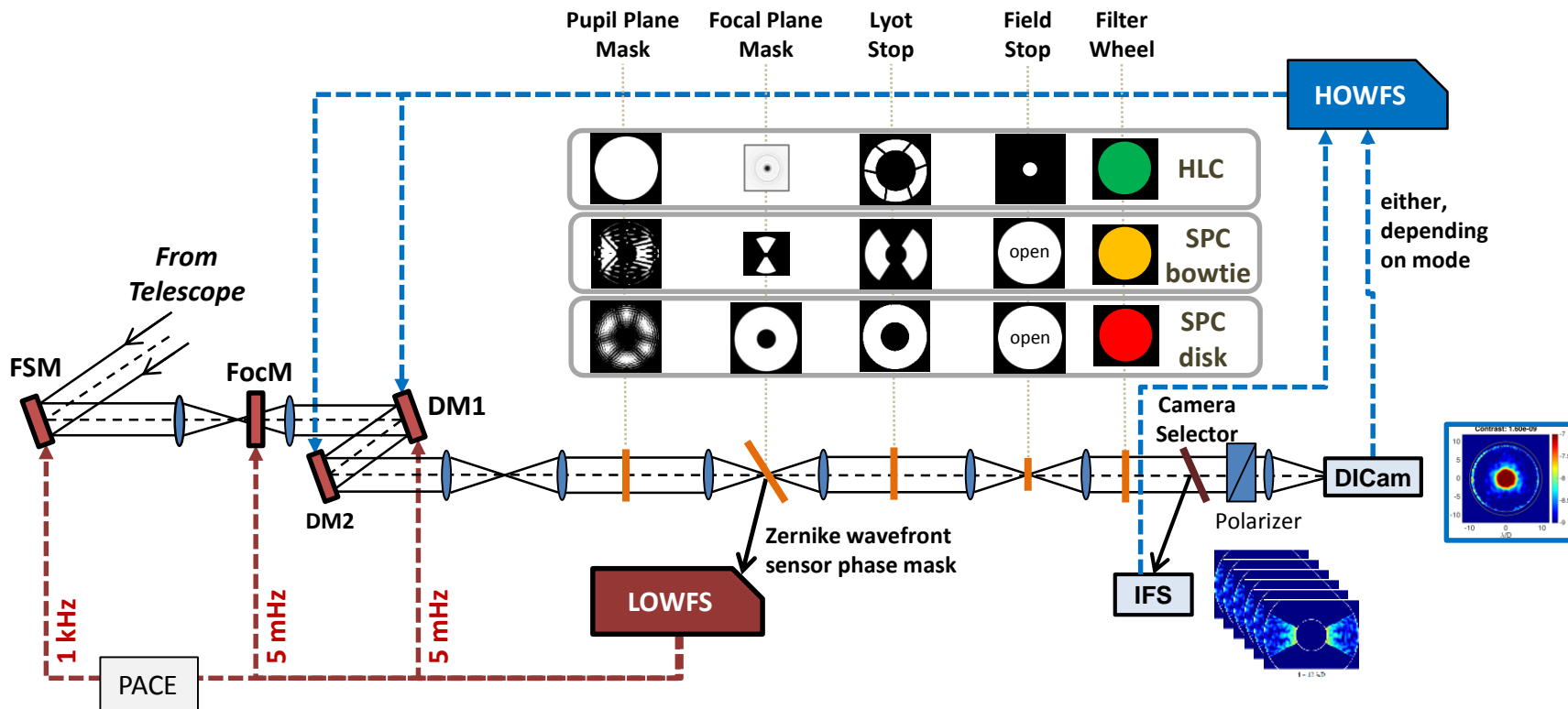
- Two selectable coronagraph technologies (HLC, SPC)
- Two deformable mirrors (DMs) for high-order wavefront control
- Low-order wavefront sensing & control (LOWFS&C)

September 2018

- Direct imaging camera (DICam)
- Integral field spectrograph (IFS, R = 50)
- Photon-counting EMCCD detectors

Coronagraph Elements

λ₁=575 nm, 10%   λ₂=660 nm, 18%   λ₃=760 nm, 18%   λ₄=825 nm, 10%

Hybrid Lyot Coronagraph
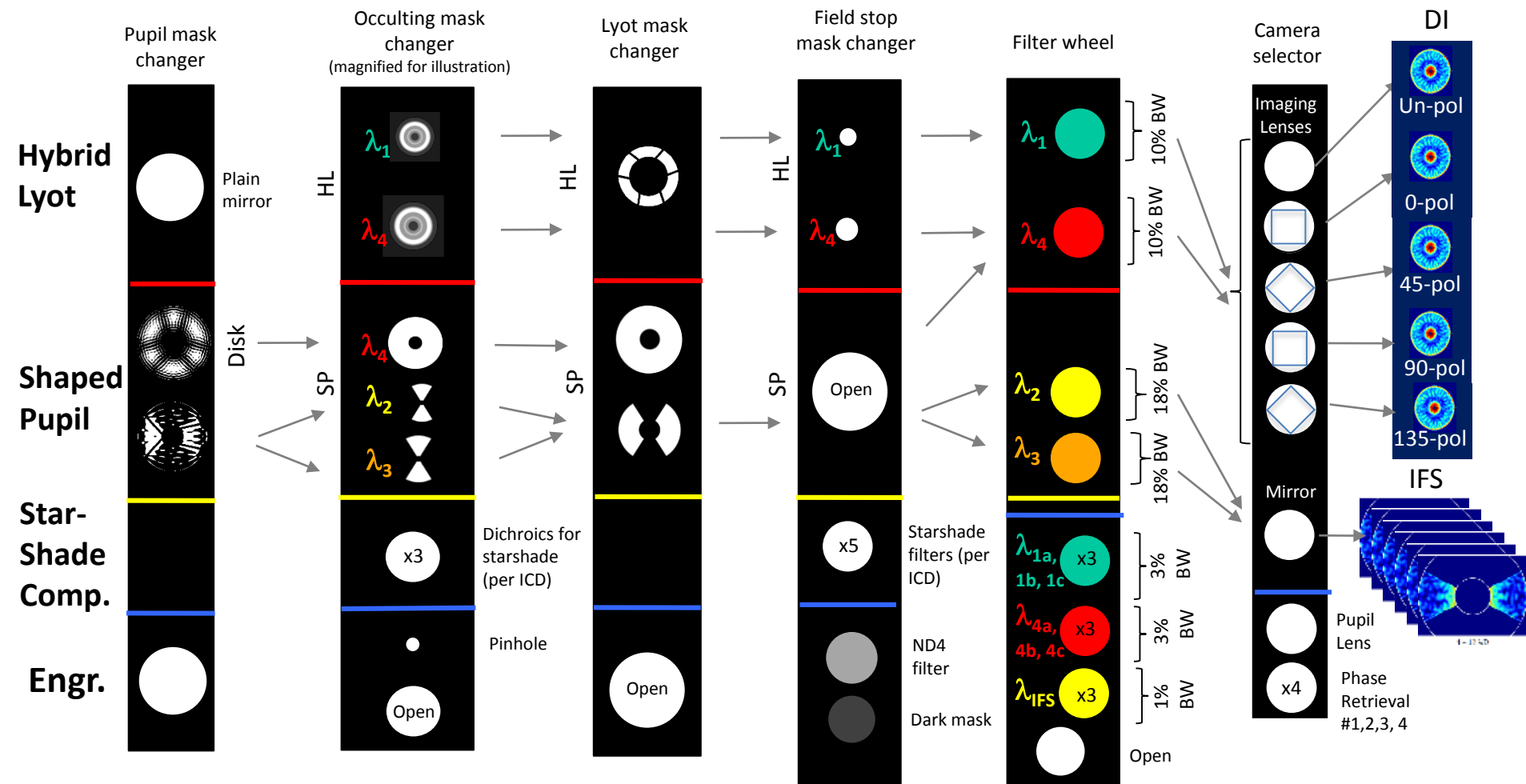
- The HLC provides a full 360° high contrast field of view.
- Focal plane occulting mask is a circular, r = 2.8 λ_c/D partially-transmissive nickel disc overlaid with a dielectric layer with a radially and azimuthally varying thickness profile.
- The HLC design incorporates a numerically optimized, static actuator pattern applied to both deformable mirrors.
- Lyot stop is an annular mask that blocks the telescope pupil edges and struts.
- September 2018 updated design PSF core throughput is 5.2% relative to the energy incident on primary mirror (ignoring losses from reflections and filters).
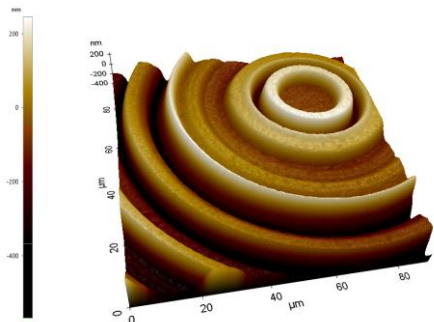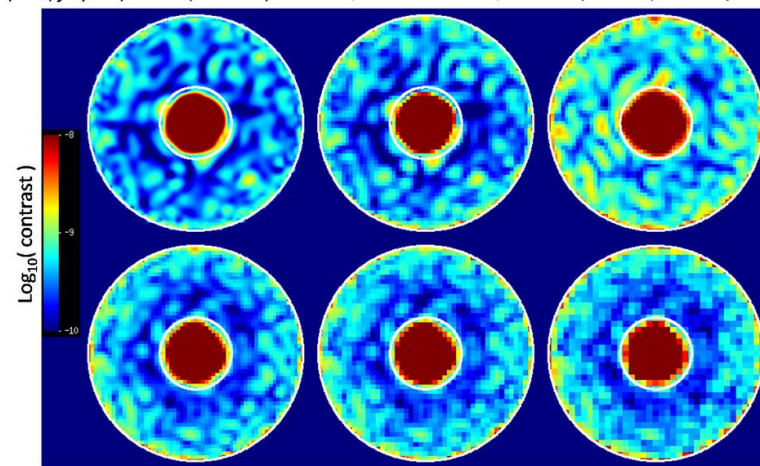

HLC occulting mask. AFM surface height measurement of an occulting mask fabricated by the JPL Micro Devices Lab. Recent design refinements include azimuthal ripples in thickness of the dielectric, which extends across the field of view.
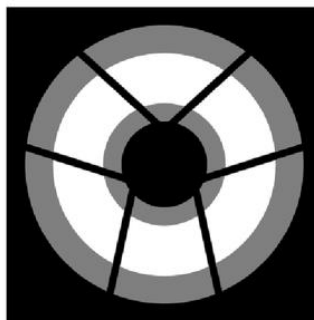
HLC Lyot stop. Diagram of Lyot stop model: white represents the transmitted region; black represents the telescope pupil; gray represents the region blocked by the stop in addition to the telescope pupil.

9 wavelengths, perfect knowledge 0.2 λ_c/D point sampling (Inner, full) = (3.8x10^{-10}, 4.2x10^{-10})	9 x 1.1% sub-bands, probing, 0.3 λ_c/D finite pixels (4.2x10^{-10}, 4.6x10^{-10})	2 x 5% sub-bands, probing, 0.3 λ_c/D finite pixels (9.0x10^{-10}, 7.8x10^{-10})
3 x 3.3% sub-bands, probing, 0.3 λ_c/D finite pixels (3.3x10^{-10}, 5.0x10^{-10})	3 x 3.3% sub-bands, probing, 0.4 λ_c/D finite pixels (3.2x10^{-10}, 5.3x10^{-10})	3 x 3.3% sub-bands, probing, 0.5 λ_c/D finite pixels (3.3x10^{-10}, 5.5x10^{-10})

Simulated HLC PSF including aberrations and high-order wavefront control operations, illustrating the annular dark zone between 3 and 9 λ_c/D. Each sub-panel represents a different scenario for DM probe wavelength resolution and detector sampling.

References
- J. Trauger, D. Moody, et al., JATIS Vol 2, id. 011013 (2016) - https://doi.org/10.1117/1.JATIS.2.1.011013
- J. Krist, et al., Proc SPIE Vol 10400, id. 1040004. (2017) - http://dx.doi.org/10.1117/12.2274792
- K. Balasubramanian, et al., Proc SPIE Vol 10400, id. (2017) - https://doi.org/10.1117/12.2274059
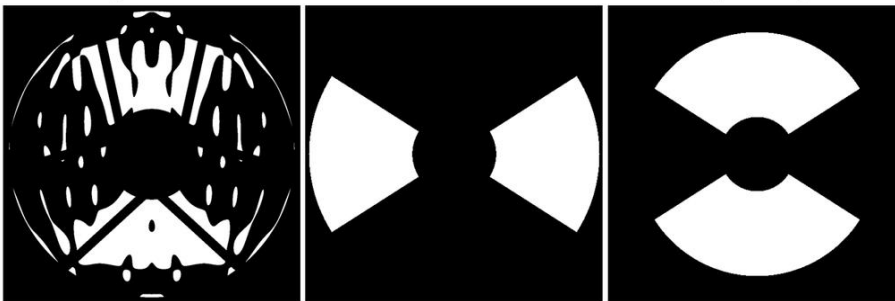
Shaped Pupil Coronagraph

- The shaped pupil apodizer is a reflective mask on a silicon substrate with aluminum regions for reflection and black silicon regions for absorption.
- The hard-edged occulting mask has either a bowtie-shaped opening for characterization (spectroscopy) mode or an annular aperture for debris disk imaging.
- The Characterization SPC designed in 2017 produces a 2 x 65° bowtie dark zone from 3 – 9 λ_c/D over an 18% bandpass, and has a PSF core throughput of 3.8% relative to the energy incident on primary mirror (ignoring losses from reflections and filters).
- The Debris Disk SPC design produces a 360° dark zone from 6.5 – 20 λ_c/D in a 10% bandpass.

Pupil Mask   Focal Plane Mask   Lyot Stop

Characterization shaped pupil coronagraph masks from 2017. Design by A. J. E. Riggs.

λ_c = 660 nm, No polarization errors, No jitter

λ_c = 660 nm, With polarization errors, No jitter

λ_c = 660 nm, With polarization errors, 1.6 mas RMS jitter

λ_c = 770 nm, With polarization errors, No jitter
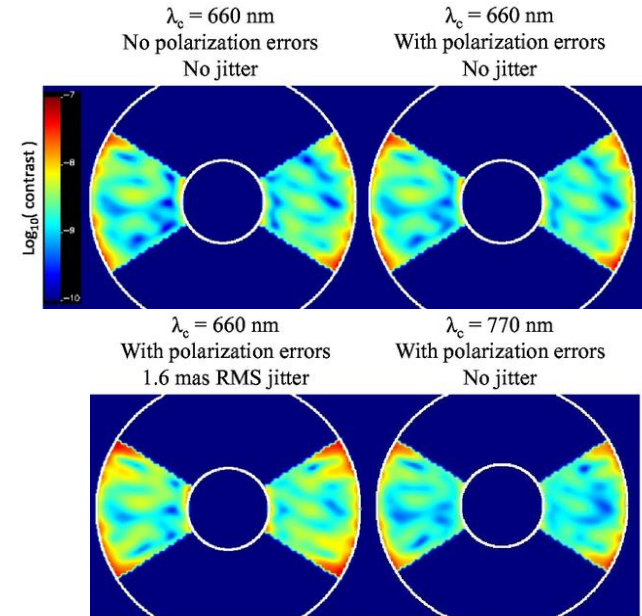
Characterization SPC simulations at λ_c = 660 and 770 nm including system aberrations, pointing jitter, and wavefront control operations. The circles correspond to r = 3 and 9 λ_c/D.

References
- N. T. Zimmerman, et al., JATIS Vol 2 id. 011012 (2016) - http://dx.doi.org/10.1117/1.JATIS.2.1.011012
- K. Balasubramanian, et al., JATIS Vol2 id. 011005 (2015) - https://doi.org/10.1117/1.JATIS.2.1.011005
- A. J. E. Riggs et al., N. T. Zimmerman, et al., Proc SPIE Vol 10400 (2017) - http://dx.doi.org/10.1117/12.2274437
- J. Krist, et al., Proc SPIE Vol 10400, id. 1040004. (2017) - http://dx.doi.org/10.1117/12.2274792

Wavefront Control

- The baseline CGI design includes four active optics to control the wavefront: a **fast steering mirror** (FSM), a flat **focusing mirror** (FocM), and two **deformable mirrors** (DM 1 and DM 2) with 48x48 actuators each.

- High-order wavefront control is implemented by the Electric Field Conjugation (EFC) method. The EFC loop operates on science focal plane data by measuring the interaction of aberrated on-axis starlight with a sequence of DM actuator probes.

- Pointing, focus, and low-order wavefront drifts are sensed by the **Low-Order Wavefront Sensing and Control** (LOWFS/C) subsystem using the Zernike phase-contrast technique on starlight rejected from the occulting mask. Corrections to Zernike modes Z5—Z11 are applied to DM 1.

- The FSM control loop corrects line-of-sight pointing jitter to below 0.8 milliarcsec.
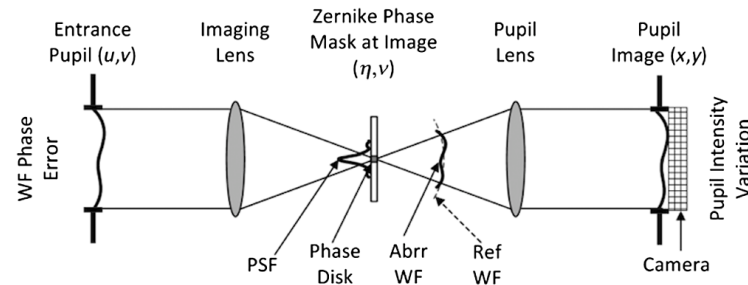
Conceptual diagram of the Zernike phase contrast wavefront sensor (F. Shi, et al., 2016).
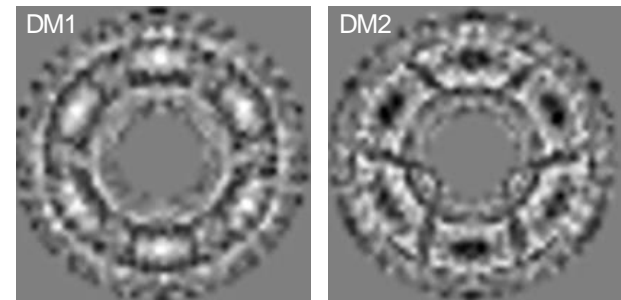

Optimized DM surfaces applied in HLC data simulations.

References
- T. Groff, A. J. E. Riggs, et al., JATIS Vol 2, id 011009 (2015) - https://doi.org/10.1117/1.JATIS.2.1.011009
- F. Shi, et al., JATIS Vol 2, id 011021 (2016) - https://doi.org/10.1117/1.JATIS.2.1.011021
- J. Krist, et al., JATIS Vol 2, id 011003 (2015) - https://doi.org/10.1117/1.JATIS.2.1.011003

- Electron Multiplying CCD (EMCCD) technology is advantageous for a coronagraph application.
  - Programmable gain provides wide dynamic range suitable for bright scenes expected during acquisition and coronagraph configuration, while photon counting capability can be used for faint light observations with zero read noise.
- EMCCD detectors are baselined for direct imaging, spectroscopy and wavefront sensing applications in CGI.
  - Subarray readout suitable for a wavefront sensor application enables 1000 frame-s^{-1} operation to accommodate tip-tilt sensing.
- Work at JPL is focused on low flux characterization with radiation damaged sensors.
  - JPL is investing in modifications to the commercial version of the EMCCD that are expected to improve margins against radiation damage in a flight environment. Characterization of flight prototype devices is planned for FY19.
- JPL's EMCCD test lab has measured a low flux threshold of 0.002 c-psf^{-1}-s^{-1}, equivalent to a 32.4 magnitude star through a 2.4m telescope at 500 nm with 10% bandwidth.
  - Devices irradiated to 5 years equivalent life at L2 meet coronagraph technology requirements. Low flux QE is reduced 20-25% and dark current is increased ~2x.

Radiation-hardened EMCCDs are in Production

Commercial EMCCD

Flight Prototype EMCCD
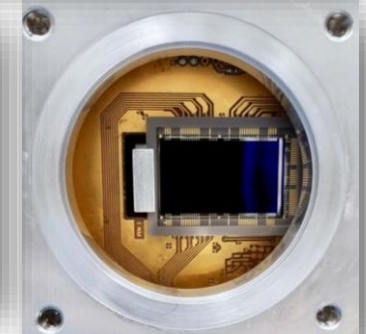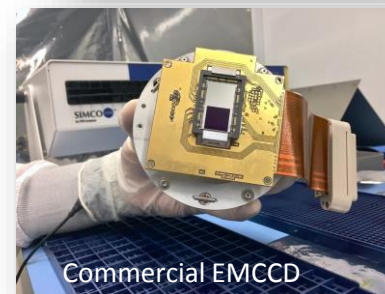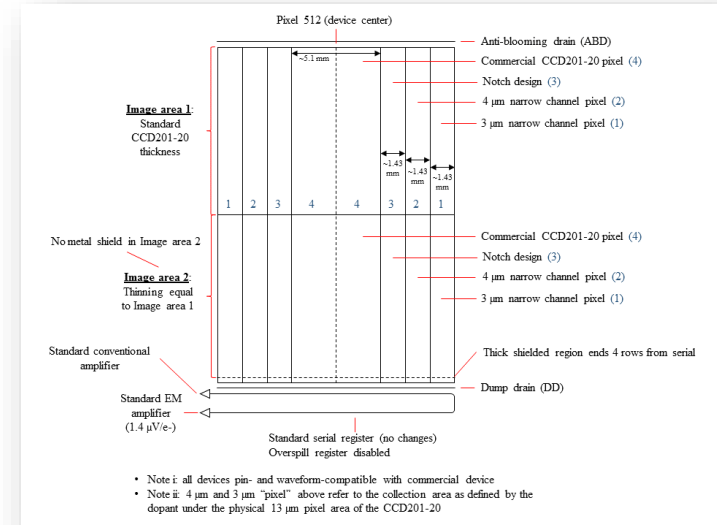
References
- L. Harding, R. Demers, et al., JATIS Vol 2, id 011007 (2016)

13

- Lenslet-based integral field spectrograph (IFS) with R=50 spectral resolving power and a 1.6-arcsec field of view.

- A reflective relay feeds a lenslet array, which critically samples the coronagraph image (2 lenslets per λ_c/D at 660 nm). The light from each spatial element is dispersed by a prism group.

- The prioritized spectroscopy demonstration filter is an 18% bandpass centered at 760 nm (CGI Science Band 3) matched to the characterization SPC. However, by design the IFS can capture an instantaneous bandpass up to 20% anywhere in the range 600 to 1000 nm.
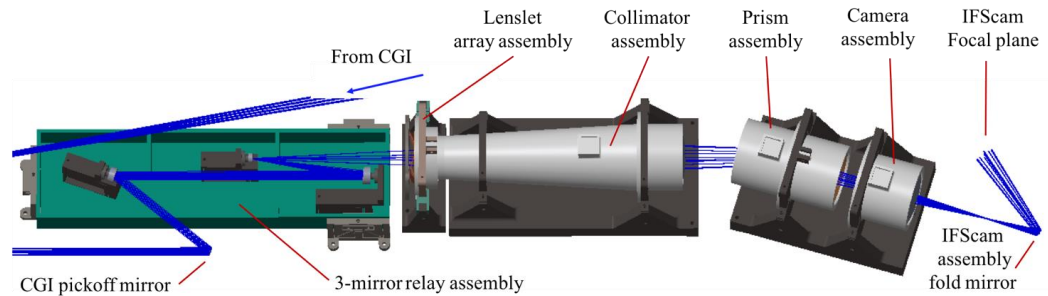
Baseline opto-mechanical layout of the CGI IFS, showing the beam progression through the relay mirrors, lenslet array, collimator, prism, and reimaging optics. The spectra are focused on a dedicated EMCCD detector (the IFScam; not shown).
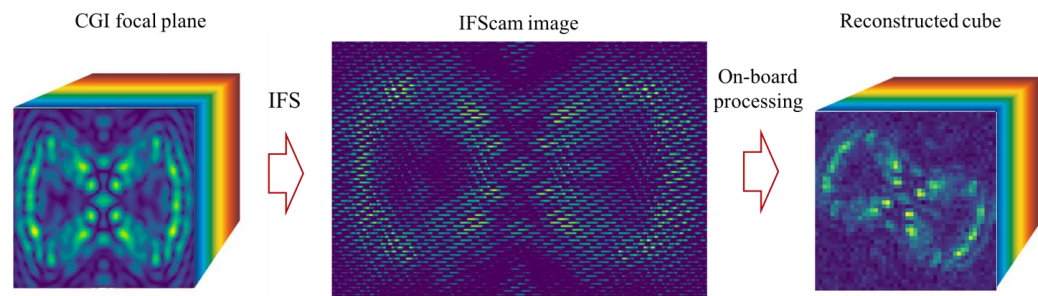
The IFS produces a spectrally dispersed map of the CGI focal plane, comprised of a grid of interleaved microspectra. There is one microspectrum for each lenslet, or spatial element (center). A wavelength-resolved data cube (right hand side) is reconstructed by software.

References
- M. McElwain, A. Mandell, Q. Gong, et al., Proc SPIE Vol 9904 (2016)
- M. Rizzo, T. Groff, N. Zimmerman, et al., Proc SPIE Vol 10400 (2017)
- A. Mandell, T. Groff, Q. Gong, et al., Proc SPIE Vol. 10400 (2017)

Results from the Occulting Mask Coronagraph (OMC) Testbed at JPL HCIT

Normalized intensity maps measured on the OMC testbed in broadband (10 %) light for SPC (left) and HLC. The total contrast between 3 – 9 λ/D is listed on top of each figure.

Dynamic contrast demonstration with a Low Order Wavefront Sensing and Control (LOWFS/C) system integrated on the Occulting Mask Coronagraph testbed. When line-of-sight disturbances and low order wavefront drift (slow varying focus) are introduced on the testbed, the LOWFS senses the pointing error and wavefront drift and corrects them by commanding a fast steering mirror and one of the DMs. Demonstrations with both the SPC and HLC masks surpassed their 1E-8 contrast goal (F. Shi, et al., Proc SPIE Vol 10400, 2017).

References
- F. Shi, E. Cady, et al., Proc. SPIE Vol 10400 (2017) - http://dx.doi.org/10.1117/12.2274887
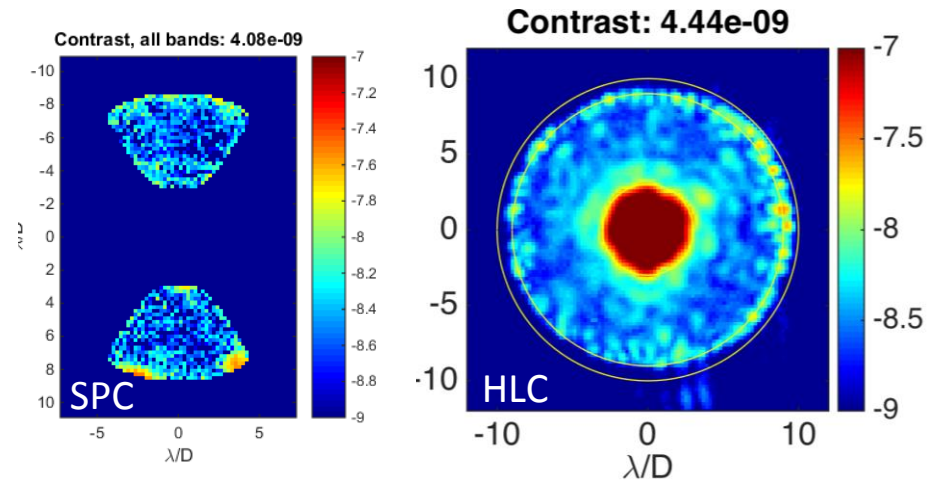- E. Cady, K. Balasubramanian, et al., Proc. SPIE Vol 10400 (2017) - http://dx.doi.org/10.1117/12.2272834
- B.-J. Seo, E. Cady, et al., Proc SPIE Vol 10400, 10.1117/12.2274687 (2017) - http://dx.doi.org/10.1117/12.2274687
- F. Shi, et al., Proc. SPIE Vol 10698 (2018) - https://doi.org/10.1117/12.2312746
- B.-J. Seo, et al, Proc. SPIE Vol 10698 (2018) - https://doi.org/10.1117/12.2314358
- D. Marx, et al, Proc. SPIE Vol 10698 (2018) - https://doi.org/10.1117/12.2312602

Operations Concept: autonomous steps

Prepare for Observation
- Set DM and let settle (WFI concurrent)
- Thermal setting

Acquire Reference Star
- Send CGI sensed error to observatory
- LOWFSC locks on star

Set up for Dark Hole
- Set Masks, Filter
- LOWFSC zeroes T/T, Focus, LO WFE

Generate Dark Hole w/ Ref. Star
- Probes & Pairwise Estimation
- HOWFSC for DM setting

Reference Bright star

RDI

Target star and planet **2**

star chop

Acquire Target Star
- ACS move
- FOC, DM1,2 frozen

Observe Target + Roll Chop
- T/T, FocM, DM1 to DH values
- LOWFSC corrections

Acquire Reference Star
- ACS move
- FOC, DM1,2 Frozen

Observe Reference
- Single Roll state

Data to Ground for Post Proc.

- Initial alignments and generation of the high-contrast "dark hole" are accomplished with reference to a bright star.
- Target star is acquired and science observations commence.
- Dark hole is maintained via periodic revisits of the bright reference star.
- Planet signal is separated from the background speckle field via reference difference (RDI) and angular difference (ADI) imaging.
- Routine observing sequences are carried out autonomously.

- Investigations on algorithms for CGI data post-processing have encompassed both end-to-end data simulations and analysis of laboratory testbed data.
- *Reference differential imaging* (RDI) trials have probed a range of wavefront stability and noise scenarios. Simulations with spacecraft rolls have also enabled tests of *Angular differential imaging* (ADI).

1. Post-processing trials on HLC data simulations

47 UMa -13° Raw, roll 1
47 UMa +13° Raw, roll 2
β UMa Raw, ref.

Class. PSF Sub   KLIP 30 modes
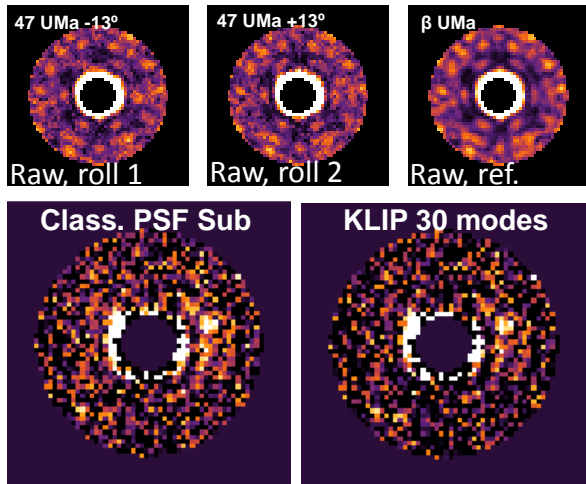
2. Post-processing trials on Laboratory Data

Raw SPC image

KLIP-subtracted, match-filtered w/ fake planet

Recovered point source
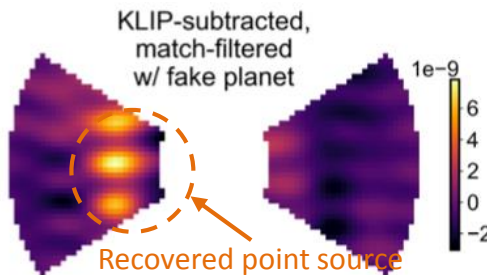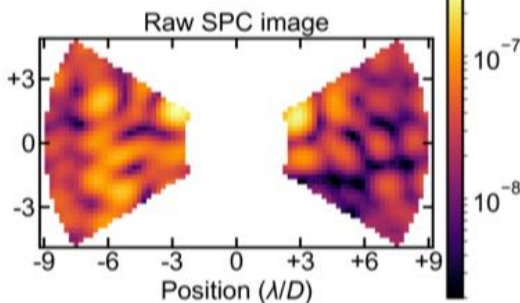
Example application of RDI to SPC data from the HCIT, demonstrating the match-filtered recovery of a fake point source inserted into one image.
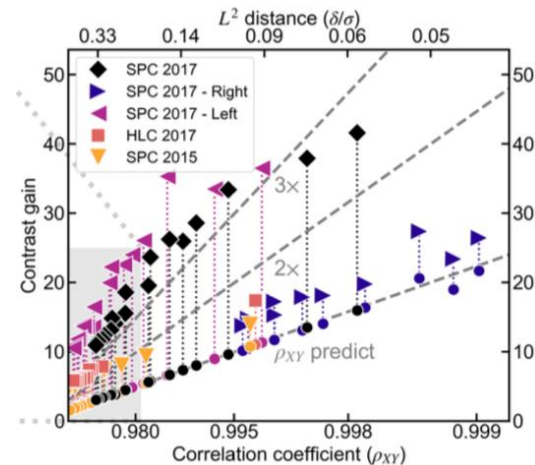
Post-processing contrast gain plotted against reference library correlation for five datasets. Above a certain correlation coefficient, the post-processing gain is comparable to the gain from classical PSF subtraction.

References
- N. Zimmerman, L. Pueyo, R. Soummer, B. Mennesson, JATIS submitted.
- M. Ygouf, N. Zimmerman, L. Pueyo, R. Soummer, et al., Proc. SPIE Vol 9904 (2016) - http://dx.doi.org/10.1117/12.2231581
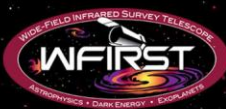
- The WFIRST baseline design is starshade-ready, to support exoplanet observations with an external starshade occulter in the event that one is launched in the future.

- CGI has 3 starshade-dedicated dichroic Zernike sensor masks in the occulter wheel to enable lateral starshade position sensing using the LOWFS camera.

- CGI has 5 dedicated filters for scientific observations with a starshade, suitable for both the direct imaging and IFS cameras.

Starshade filters

λ (nm)	BW	Δλ	λ_{min} (nm)	λ_{max} (nm)	mode
488.5	26.0%	127	425	552	img
707.5	26.1%	185	615	800	img
728	19.8%	144	656	800	IFS
884.5	26.1%	231	769	1000	img
910	19.8%	180	820	1000	IFS

These filters accommodate observations with a potential future starshade probe mission. They are held in the CGI Field Stop changer (column 4 of the mask-filter schematic in slide 6).

Starshade probe concept study reports available at
https://exoplanets.nasa.gov/exep/studies/probe-scale-stdt/

CGI Program Level Technology Objectives

- ## *Coronagraph with Active Wavefront Control*

The CGI will demonstrate coronagraphy in space with an obscured aperture and active wavefront control. WFIRST would fulfill this objective by detecting a companion object next to a star, on at least two stars, at a contrast level and separation that requires a functional coronagraph and wavefront control capability.

- ## *Coronagraph Elements*

The CGI will advance the engineering and technical readiness of key coronagraph elements needed for future missions capable of detecting and characterizing Earthlike planets. These elements include coronagraph masks, low-order wavefront sensors, high actuator count deformable mirrors, low noise detectors, and integral field spectrographs. WFIRST would fulfill this objective by demonstrating in-space operation of the elements listed.

- ## *Advanced Coronagraph Algorithms*

The CGI will support development and in-flight demonstration of coronagraph software that could enhance the capability or simplify the architecture of future missions. WFIRST would fulfill this objective by demonstrating the ability to modify the wavefront sensing and control algorithms during the prime science mission.

- ## *High Contrast Performance Characterization*

WFIRST will perform measurements that characterize the integrated performance of the coronagraph and observatory as a function of time, wavelength, and polarization. WFIRST would fulfill this objective by gathering data on a target star that enables in-flight performance characterization of the coronagraph, including a revisit of the target and a repointing maneuver.

- ## *High-Contrast Data Processing*

The CGI will demonstrate advanced data processing and analysis techniques required to identify, spectrally characterize and distinguish astronomical sources in the presence of instrumental and astrophysical background noise at high contrast. WFIRST would fulfill this objective by producing photometric, astrometric, and spectrographic measurements of astrophysical object(s), including at least one point source and at least one extended object.

NASA envisions a CGI Participating Scientist Program (PSP)

- *To guide science program in the years following the formal technology demonstration*
- *The PSP to be embedded with the CGI project prior to launch*
  - *Science objectives could include:*
  - *~double the number of planets with imaging and spectroscopy*
    - *More than double the number of imaged disks*
  - *~3 months for a search for new planets*
  - *Could discover ~10 new Jupiter analogues*
  - *May discover a few Neptunes or mini-Neptunes*
    - *Investigate ~20 highest priority systems for exo-Earth missions*
    - *Exo-Earth imaging needs relatively "clean" (low dust) systems*
    - *Search for Jupiter analogues in systems with poor RV constraints*
  - ***Expanded science areas & possible GO program***
  - *New community-driven exoplanet & disk science*
  - *General astrophysics, AGNs, evolved stars…*
  - *Possible starshade rendevous*

CGI References

Reference	URL	Year
Wide-Field Infrared Survey Telescope-Astrophysics Focused Telescope Assets (WFIRST-AFTA) 2015 Report by the Science Definition Team (SDT) and WFIRST Study Office	https://wfirst.gsfc.nasa.gov/science/sdt_public/WFIRST-AFTA_SDT_Report_150310_Final.pdf	2015
Journal of Astronomical Telescopes Instruments and Systems, Vol. 2, No. 1, *Special Section on WFIRST-AFTA Coronagraphs*, eds. Olivier Guyon and Motohide Tamura	https://www.spiedigitallibrary.org/journals/Journal-of-Astronomical-Telescopes-Instruments-and-Systems/volume-2/issue-01#Editorial	2016
SPIE Proceedings Vol. 10400, *Techniques and Instrumentation for Detection of Exoplanets VIII*, ed. Stuart Shaklan	https://www.spiedigitallibrary.org/conference-proceedings-of-spie/10400	2017
SPIE Proceedings Vol. 10698, *Space Telescopes and Instrumentation 2018: Optical, Infrared, and Millimeter Wave, WFIRST I, II, III*	https://www.spiedigitallibrary.org/conference-proceedings-of-spie/10698	2018
Community White Papers submitted to the NAS Exoplanet Science Strategy Committee, co-chairs D. Charbonneau & S. Gaudi. Among the CGI-related papers are: Kasdin et al., Bailey et al., Mennesson et al., Marley et al., B. Crill et al., and others.	http://sites.nationalacademies.org/SSB/CurrentProjects/SSB_180659	2018